

# Autonomous Lunar Investigation and Communications Explorer (A.L.I.C.E.): Conceptual Design of Lunar Rover with Autonomous Capabilities

Sohini Gupta<sup>1</sup> and Adeel Khalid<sup>2</sup>

*Kennesaw State University, Marietta, Georgia, 30060, U.S.*

The present paper describes the development of the Autonomous Lunar Investigation and Communications Explorer (A.L.I.C.E.). The A.L.I.C.E. is a lunar rover design concept tailored for enhanced lunar exploration while minimizing human intervention. The rover must follow a set of requirements, ensuring its survivability on the Moon. The design of A.L.I.C.E. was specialized to account for Clavius Crater being the landing point and mission area. Details of this paper include its mission profile, thorough explanations of the process of selecting optimal instruments, CAD models of A.L.I.C.E. with descriptions of each view, and calculations regarding weight and power consumption of the rover. The rover will be used to collect lunar soil samples. These samples will be stored in an on-board compartment and brought back to the base station. Results and analysis of the model tested in simulation are also discussed. By reducing human intervention and increasing scientific data collection capabilities, this concept offers a significant leap forward in lunar surface exploration, potentially paving the way for future space missions and scientific discoveries.

## I. Nomenclature

$m$	=	mass
$D$	=	density
$V$	=	volume
$F$	=	force
$a$	=	translational acceleration
$N$	=	Newtons
$kg$	=	kilograms
$mm$	=	millimeters

**Keywords:** Lunar rover, design iterations, lunar rover design requirements, autonomous lunar rover concept

## II. Introduction

Over the last several decades, unmanned vehicles have been sent to further develop our understanding of planetary surfaces. In recent years, there has been a resurgence of interest in lunar exploration, with the goal of expanding on scientific investigations. An essential component is the progress of autonomous rovers, which are capable of navigating and exploring the lunar surface without constant human interference. The design of an autonomous lunar rover should encompass several elements such as mobility, energy storage, communication, scientific instruments, and autonomous capabilities. Each aspect plays a critical role in navigating safely in the lunar terrain and gathering scientific data. The unique conditions of the Moon, such as an extreme range of temperatures, rugged surface, and limited resources, necessitate innovative solutions to ensure the vehicle's reliability, longevity, and adaptability. The rover must also be capable of efficiently utilizing available power sources, communicating with Earth, and operating autonomously to carry out mission objectives. Through a thorough examination of existing mission concepts and insights from previous rover missions, this paper will delve into the technical and operational aspects of an autonomous lunar rover. By analyzing and synthesizing current research, an optimal design framework for the rover's capabilities can be proposed for lunar exploration. The development of an autonomous rover provides a significant leap forward in lunar exploration. This research will contribute to the existing body of knowledge by introducing a design concept that addresses the technical, operational, and scientific aspects of such a vehicle. It is aimed to facilitate the advancement of lunar exploration and pave the way for new ideas on the Moon.

---

<sup>1</sup> Student (High School)

<sup>2</sup> Professor, Industrial & Systems Engineering, and AIAA Life Member Grade

### III. Literature Review

Over the years, numerous rover design studies have been conducted focusing on various aspects of the vehicle. James Zakrajsek provides a comprehensive overview of various design concept proposals designed for future Moon and Mars missions, built on the reviews of past missions [1]. For each concept, they highlight the key features, challenges, and potential benefits, offering valuable insight for the development of advanced exploration.

Simon Kassel presents a breakdown of the Russian lunar-exploration vehicle, Lunokhod-1, providing information on its structure, automation, operation, and other relevant data [2].

V. Gromov considers the features of design, benefits, and results of the Russian Lunokhod-2 mission [3]. They pay particular attention to the chassis, which has allowed the rover to traverse at significant cross-country distances and investigate the lunar surface.

Brian Wilcox analyzes the performance of the Sojourner rover, which landed on Mars on July 4th, 1997 [4]. This includes its telemetry, commands, and images, contributing to the understanding of its pros and cons, and the progress of rover design.

Mark Maimone presents a complete review of the twin Mars rovers Spirit and Opportunity, and more specifically, their autonomous navigation capabilities [5]. They depict the benefits of the rovers' mobility and navigation, giving the ability to use the concepts for designs in the near future.

Joy Crisp provides insight into the mission, purpose, and goals of the twin rovers (Spirit and Opportunity) [6]. Along with its purpose, they describe the instruments being used and their placements, Entry, Descent, and Landing (EDL), and other parts of the rovers' path.

J. Purvis discusses the design process and prototype performances of a rover that could potentially be used on the Moon, but has only been tested terrestrially [7]. They explore how the design decisions were derived, what problem(s) they may assist with, and the benefits and risks of each.

Wendy Amai discusses the development of a prototype of the RATLER project, started in 1993 [8]. They list the weaknesses of the design, and proposals on how to address them, providing considerations to make in upcoming projects.

NASA provides a brief summary of the Yutu-2 rover on the Chang'e 4 mission, including its mass, dimensions, and instrumentation [9].

Justin Maki extensively examines each of the ten types of cameras used in the Spirit and Opportunity rovers, including the Hazard Avoidance cameras, Navigation cameras, and the Descent camera [10]. A detailed evaluation of these cameras allows the comparison and consideration of features that should be used for optimal performance.

Javier Gómez-Elvira offers a detailed description of the Rover Environmental Monitoring Station (REMS) component, which measures UV radiation, atmospheric pressure, air and ground temperature, humidity, and wind on Mars [11]. Through the data sets, they give perception to the efficiency of the instruments in use.

Javier Gómez-Elvira heavily discusses the benefits of the sensor group and the mixture of purposes that contributes to its importance [20]. They describe in detail each of the sensors that constitutes REMS scientific potential their data can hold.

NASA characterizes the Radiation Assessment Detector (RAD), a sensor on the Mars rover Curiosity to measure radiation in the environment [36].

Steven Squyres explores the purpose and results of the suite of scientific instruments on the Spirit and Opportunity rovers, entitled the Athena Payload [12]. For each instrument, it features the primary scientific objectives, functionality, and design, developing understanding to increase the possibility for further improvement.

Martin Schrön describes the applications of Cosmic Ray Neutron Sensing (CRNS), a concept for measuring soil moisture in fields in a non-invasive manner [13]. This concept could have potential applications used in extraterrestrial environments.

Jim Bell discusses the camera system, called Mast Camera (Mastcam), on the Curiosity rover [14]. They point out the calibration process, the benefits of the calibration process, its results, and key characteristics of the camera system.

J. A. Rodriguez-Manfredi assesses the Mars Environmental Dynamics Analyzer (MEDA), a sensor suite to analyze the Martian environment, on the Perseverance rover [15]. They also provide a comparison to previous environmental monitoring payloads.

Daniel McCleese considers the Mars Climate Sounder experiment held on the 2005 Mars Reconnaissance Orbiter which attempted to characterize the Martian atmosphere and climate with the same precision of terrestrial weather satellites [16]. They compare the instruments' benefits and disadvantages, giving an overall overview of its efficiency.

Rajeshuni Ramesham includes an extensive overview of Platinum Resistance Thermometers (PRT) used on the Curiosity rover which monitors the temperature of its electronics [17]. They emphasize the criticality of sensors to the health of the hardware during the mission life cycle.

Gaetano Quattrocchi explains the instrumentation on the Curiosity rover that has the purpose of regulating the temperature within its parts [18]. For each instrument, they provide a detailed summary of the attributes, mechanisms, and functionality.

Ramona Gaza discusses the advantages of the Battery-operated Independent Radiation Detector (BIRD), and in addition, makes a comparison of the instrument to the radiation area monitor (RAM) [19].

Dirk Schmanke gives a general summary of the experimental purposes and features of the Alpha Particle X-Ray Spectrometer (APXS) sensor head, as well as its experimental results [31].

NASA briefly synthesizes information on the Rock Abrasion Tool as used on the MER-A rover, also known as Spirit, including the tool's qualities such as mass, dimensions, power usage, and scientific benefits [32].

The Analyst's Notebook, produced by NASA's PDS Geosciences Node, comprises of a comprehensive overview of the Mössbauer Spectrometer (MB) used to obtain the mineralogical information of rock, soil, and dust on Mars by the Mars Exploration Rover missions [33]. The overview considers information on its objectives, calibration, operational considerations, and the electronics used.

Rao Surampudi proposes an extremely thorough review of the various energy storage technologies that could potentially be used in extraterrestrial missions [21]. Along with a thorough review, there are insightful comparisons for each type of technology which provides more knowledge when deciding the optimal product.

Patrick Peplowski reports the performance of the Neutron Spectrometer System (NSS) through a science calibration campaign, describing its purpose and benefits [35]. The NSS is used in the concept of the VIPER lunar rover.

Jack Mondt assesses the potential of advanced energy storage technologies to enhance future missions [34].

F. C. Krause evaluates commercial Lithium-Ion battery cells, delving into the design, production, and capabilities of each type [22]. Through the consideration of several experiments and missions in which the cells were used, they synthesize the information into the ideal Li-ion cells available to use in prospective space missions.

John-Paul Jones provides a summary of batteries that have been used in both past, current, future, and concept robotic spacecraft missions, evaluating the extent to which the battery contributes to the efficiency of the robot [23]. They specifically focus on the missions operated by the National Aeronautics and Space Administration (NASA) Jet Propulsion Laboratory (JPL).

Ratnakumar Bugga provides insight into the optimal energy storage technologies for numerous mission types such as landers and rovers, orbiters, and probes [24].

Florian Cordes reviews the design of the rover Sherpa, focusing on the mechanical design process of its suspension system, and discussing the achievements and drawbacks of such a design [25].

Stephen Gerds covers the design and development of the Lunar Rover Optimization Platform (LROP) targeted for medium class rovers [26]. They analyze the several wheel design experiments that have been conducted, strengthening the platform's abilities.

David Braun describes the design, test, and results of the development of a DC brush motor specifically for longer duration operations in low temperature, built off of past challenges faced with DC brush motors [27].

L. K. Ding details the results of the exploration experiments conducted by the Yutu-2 rover on the lunar surface, examining the rover path, physical properties of the same path, and scientific investigations that were carried out along with the instrumentation used for the investigations [28].

T. V. Torchynska assesses the options for high efficiency solar cells and compares the most popular choices, giving the advantages and disadvantages of each Si, GaAs, InGaP, and InP solar cell [29].

Geoffrey Landis discusses the potential advantages for advanced solar arrays to be used in future Mars missions [30]. Several test results of solar cell technologies operating under Mars conditions are presented and analyzed, taking into account the environmental challenges that the solar array operation faces.

Inspired by these and other ideas, a new lunar rover A.L.I.C.E. is designed in the present study.

## IV. Methodology

In this section, the process through which A.L.I.C.E. is conceptualized and designed are discussed. The criteria, constraints, and goals are explained thoroughly and broken down into different parts.

### A. Requirements

A.L.I.C.E. is designed to satisfy the following system-level requirements.

1. The A.L.I.C.E shall measure lunar and surrounding temperature
2. The A.L.I.C.E shall measure the radiation levels
3. The A.L.I.C.E shall determine soil composition
4. The A.L.I.C.E shall measure moisture content of lunar soil
5. The A.L.I.C.E shall collect samples of the lunar surface
7. The A.L.I.C.E shall navigate through rough terrain, specifically the lunar surface
8. The A.L.I.C.E shall physically observe its surroundings
10. The A.L.I.C.E shall not exceed 3m x 3m x 3m
12. The A.L.I.C.E shall have a clearance of 10cm-20cm
13. The A.L.I.C.E shall carry and transport various samples
16. The A.L.I.C.E shall not exceed a dry mass of 800kg
17. The A.L.I.C.E shall travel in the range of 20-40 km
18. The A.L.I.C.E shall maintain stability while navigating rough terrain
19. The A.L.I.C.E shall not exceed a top speed of 0.2mph
20. The A.L.I.C.E shall survive through the lunar temperature swings of -130C to 120C

**B. Mission Profile**

The Mission Profile of A.L.I.C.E. consists of phases which it could potentially perform in, including its duration and location. A map is present to assist with visualizing the rover’s path.

T = time 1 day = 1 Earth day (morning & night)  
D = distance 1 Lunar day (equivalent to morning) = 14 Earth days (morning & night)

**Clavius Crater Mission**

1. land in Clavius Crater T = 0, D = 0	2. Peam picture of crater T = 10, D = 0	3. check instruments, communications, etc.	4. first drives T = day 2-3, D = 80m (in total, towards center of crater)	5. use moisture and temperature sensors T = day 4, D = 80m.
6. use soil penetrator T = day 4 + 10min	7. use spectrometer for soil composition analysis T = day 4 + 20min	8. drive T = day 4 + 1h	9. T = day 5, D = 0.52 km	steps 5-9: block 1, repeat block 1 (4x)

**Geological Exploration Mission**

10. continue driving until a rock is found, use RAT for the first time T = day 14	11. analyze composition of rock, taking high-res images T = day 14	12. lunar night day 15-28	13. leave Clavius Crater to surroundings
14. explore near Clavius, continuously using Peam, analyzing soil composition, and rock whenever there is one near T = 36-42, D = 2.5km (by the end)	15. lunar night day 42-56	steps 14-15: block 2, continue block 2 until third lunar night	

**Environmental Monitoring Mission**

16. continue exploring for around D = 0.5km (use Peam to take pictures of surroundings) T = day 85	17. use temperature and radiation sensors T = day 86, D = 8.82km (total by the end)	18. use spectrometer for atmospheric composition T = day 86 = 30min
---	--	--

19. drive = 0.5km steps 16-19: block 3  
T = day 87

20. continue to repeat the instrument usage in Blocks 2 & 3

\*continuously use camera during all stages to record surroundings once reaching a destination and for navigation  
\*in areas near the Clavius Crater, make measurements of moisture and humidity

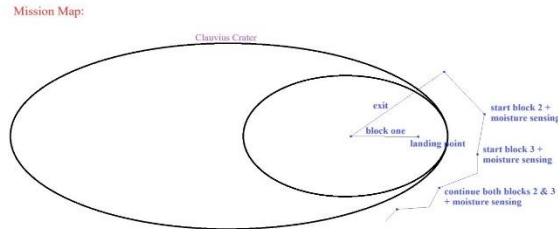


**Fig. 1 A.L.I.C.E Mission Profile**

**C. Weight Calculations**

To minimize power consumption and maximize range and endurance of A.L.I.C.E., the total mass of the rover is a crucial design consideration. Mass calculations include estimating fractional masses of its components, instrumental payload, and sample payload. The mass breakdown is given in Table 1.

**Table 2: Mass Breakdown**

Part of Rover	Total Mass (kg)
Empty Weight of Rover:	246.426
Wheels (6):	99.147
Rocker-Bogie Suspension System:	18.358
Platform:	91.089

Empty Mass of Robotic Arm:	20.158
Total Mass of Robotic Arm:	22.614
Empty Mass of Pole:	17.674
Total Mass of Pole:	21.107
Payload:	135.022
Total Mass of Rover:	381.448

#### D. COTS Components

The instruments used for the optimization of the purpose and mission of A.L.I.C.E. are listed in Table 2 below. Each instrument is carefully selected to ensure requirements and efficiency criteria are met.

Several options are considered for each component, while also factoring in advantages and disadvantages, mass, and efficiency. To find these options, past missions on both the Moon and Mars are examined in depth, and what seemed the most optimal in terms of past performance and relevance to A.L.I.C.E. are considered.

For cameras, different types are considered to ensure the safety of the rover, including for hazard avoidance, navigation, descent, and panoramic views. The capacities for each resolution at specific distances for the descent camera are specifically considered. The cameras on this list are all used in the Mars Exploration Rover mission, as well as others. Isometric view of the parameterized Computer Aided Design (CAD) models of the Microscopic Imager (MI), panoramic camera, navigation camera, descent camera, and hazard avoidance camera are shown in Figure 2 and Figure 3.

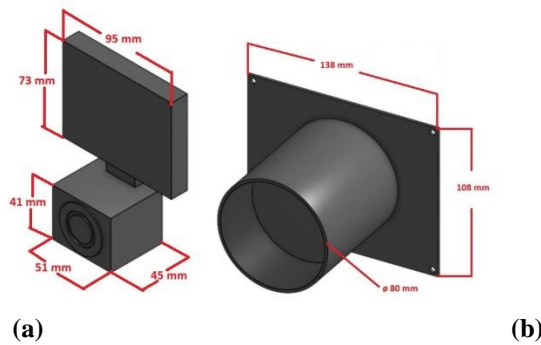


Fig. 2 (a) Isometric View of Microscopic Imager (MI) (left), (b) Isometric View of Panoramic Camera (right)

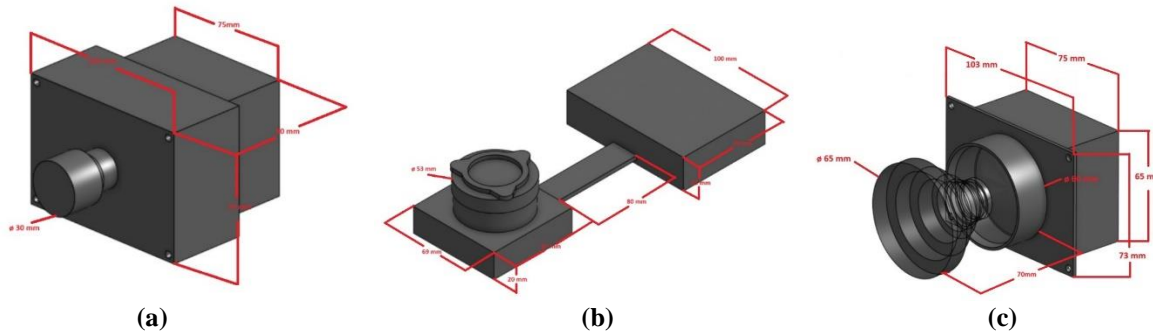
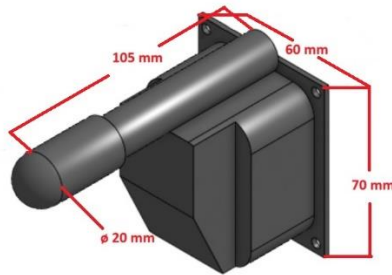


Fig. 3 (a) Isometric View Navigation Camera (top left), (b) Isometric View of Descent Camera (top right), (c) Isometric View of Hazard Avoidance Camera (bottom)

Two types of temperature sensors are used: one for environmental detection, and one to monitor the temperature of the rover's hardware. In choosing temperature sensors, the range of functionality is examined. The higher the environmental sensibility of the camera, the more valuable it is to use on the rover. The CAD model of the Environmental Monitoring System (REMS) is shown in Figure 4.



**Fig. 4 Isometric View of Rover Environmental Monitoring System (REMS)**

The radiation detectors are selected based on its the capability to measure the surface radiation levels as well as its range in bands. There are only a few available options to pick from. A CAD model of the selected Radiation Assessment Detector (RAD) is shown in Figure 5.

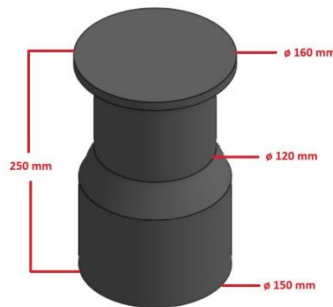


**Fig. 5 Isometric View of Radiation Assessment Detector (RAD)**

The evaluation of soil sensors is based upon the ability to detect elemental chemistry, properties of the soil, as well as sample collection of the surface. In this scenario, different sensors are used. CAD models of the Alpha Particle X-Ray Spectrometer (APXS), Mossbauer Spectrometer (MS), and the Rock Abrasion Tool are shown in Figure 6.

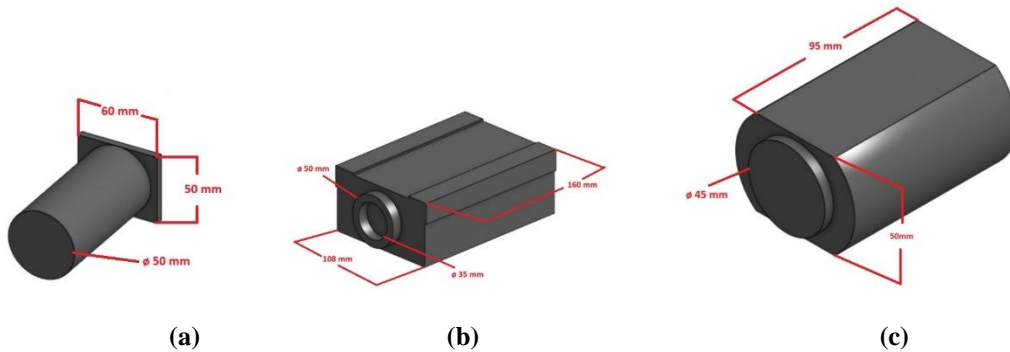


**Fig. 6 (a) Isometric View of Alpha Particle X-Ray Spectrometer (APXS) (top left), (b) Isometric View of Mossbauer Spectrometer (MS) (top right), (c) Isometric View of Rock Abrasion Tool (bottom)**

The moisture sensor should be able to detect water on a surface, both directly and indirectly. Options that meet this criteria and could work on extraterrestrial surfaces are scarce. The efficiency of the method was taken into large consideration for this instrument. CAD models were created using Onshape ® and SolidWorks ® as part of this study.

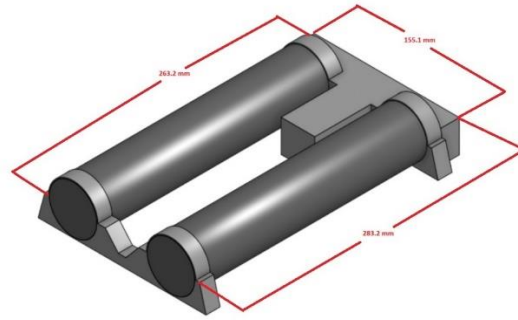


**Fig 7 Isometric View of Neutron Spectrometer System (NSS)**

Batteries, being extremely crucial to the rover's survivability, are assessed in even more depth. Efficiency, mass, and power production within a Watt-hour are registered to make sure the rover could function properly.

Solar Panels are evaluated based on their efficiency, and the one with the highest efficiency is prioritized. Along with high efficiency, it has to be made to withstand extraterrestrial environments.

**Table 2 COTS components and descriptions**

Number	Type	Name	Description
1*	Camera (Hazard Avoidance Camera)	Hazcam	<ul style="list-style-type: none"> <li>- used during the MER mission:</li> <li>- used Schott OG590, KG5, and ND1.1 filters to create red band-pass filter centered at ~650 nm</li> <li>- Optics are f-theta fish-eye lenses with a 124° x 124° horizontal, vertical &amp; 180° FOV</li> <li>- operating temperature range: -55C to 40C</li> </ul>
2*	Camera (Navigation Camera)	Navcam	<ul style="list-style-type: none"> <li>- used during the MER mission:</li> <li>- used Schott OG590, KG5, and ND1.3 filters to create red band-pass filter centered at ~650 nm</li> <li>- CCDs have full well capacities of 17000 electrons</li> <li>- Optically identical to descent camera</li> <li>- Depth of field ranges from 0.5 m to infinity (best focus at 1m)</li> <li>- operating temperature range: -55C to 40C</li> </ul>
3*	Camera (Panoramic Camera)	Pancam	<ul style="list-style-type: none"> <li>- used during the MER mission:</li> <li>- CCDs have full well capacities of 17000 electrons</li> <li>- 370° of motion in pan direction &amp; 194° in tilt direction</li> <li>- operating temperature range: -55C to 40C</li> </ul>
4**	Camera (Soil, Rock, & Surface analyzer)	Microscopic Imager (MI)	<ul style="list-style-type: none"> <li>- Close up, high resolution images of soil, rocks, and other features of surface</li> <li>- during the MER mission:</li> <li>- CCDs have full well capacities of 17000 electrons</li> <li>- 0.42 mrad/pixel angular resolution</li> <li>- 0.03 mm/pixel spatial resolution at best focus distance of 69 mm</li> <li>- operating temperature range: -55C to 40C</li> </ul>
5*	Camera (Images while landing)	Descent Camera	<ul style="list-style-type: none"> <li>- Acquire images of surface in specific altitudes</li> <li>- during the MER mission:</li> <li>- CCDs have full well capacities of 17000 electrons</li> <li>- f/12 optical system w/ 45° x 45° FOV, 60.7° diagonal FOV, angular resolution of 0.82 mrad/pixel at center</li> <li>- Broadband filter with the center at ~750 nm &amp; full width at half maximum (FWHM) of ~200 nm</li> <li>- operating temperature range: -55C to 40C</li> </ul>
6*	Temperature Sensor (Environmental Temp)	Rover Environmental Monitoring System (REMS)	<ul style="list-style-type: none"> <li>- Measure ground temp, humidity, air temp, &amp; wind</li> <li>- used in the Curiosity rover</li> <li>- Survive 1005 cycles from -130C to 15C and -105C and 40C</li> </ul>
7	Temperature Sensor (Hardware Temp)	Resistance Temperature Detectors	<ul style="list-style-type: none"> <li>- Measures temperature of electronics in rover</li> <li>- used in the Curiosity rover</li> </ul>

		(RTD) PT1000	
8*	Radiation Detector	Radiation Assessment Detector (RAD)	<ul style="list-style-type: none"> <li>- Continuously measure spectrum of high-energy radiation at the surface</li> <li>- used in the Curiosity rover</li> <li>- part of REMS</li> <li>- Range (6 bands)</li> <li>- Total Dose: <ul style="list-style-type: none"> <li>- 210-360 nm</li> <li>- max measurable irradiance: 44.7 W/m<sup>2</sup></li> </ul> </li> <li>- UVC: <ul style="list-style-type: none"> <li>- 215-277 nm</li> <li>- max measurable irradiance: 1.57 W/m<sup>2</sup></li> </ul> </li> <li>- UVB: <ul style="list-style-type: none"> <li>- 270-320 nm</li> <li>- max measurable irradiance: 6.4 W/m<sup>2</sup></li> </ul> </li> <li>- UVA: <ul style="list-style-type: none"> <li>- 315-370 nm</li> <li>- max measurable irradiance: 25 W/m<sup>2</sup></li> </ul> </li> <li>- UVD: <ul style="list-style-type: none"> <li>- 230-298 nm</li> <li>- max measurable irradiance: 5 W/m<sup>2</sup></li> </ul> </li> <li>- UVE: <ul style="list-style-type: none"> <li>- 311-343 nm</li> <li>- max measurable irradiance: 7.65 W/m<sup>2</sup></li> </ul> </li> <li>- Survive 1005 cycles from -130C to 15C and -105C and 40C</li> </ul>
9*	Soil Sensor (Elemental Chemistry)	Alpha Particle X-Ray Spectrometer (APXS)	<ul style="list-style-type: none"> <li>- Determine elemental chemistry of rocks &amp; soils</li> <li>- Examine products of water-induced erosion, sedimentation, solution, and evaporation</li> <li>- Reveal chemistry of primary crustal rocks</li> <li>- operating temperature range: -55C to 40C</li> </ul>
10**	Soil Sensor (Penetrator)	Rock Abrasion Tool (RAT)	<ul style="list-style-type: none"> <li>- Penetrate through weathered outer regions of rocks exposing fresh rocks</li> <li>- Exposed area large enough to admit APXS and Mossbauer sensors</li> <li>- Slow so that no measurable modification of rock chem or mineralogy by frictional heating is anticipated</li> <li>- Grinding materials selected so that there is no detectable contamination of rock surfaces</li> <li>- Remove cylindrical area of 4.5 cm in diameter and &gt;0.5 cm deep from rock outer surface</li> <li>- used in the MER rovers</li> <li>- operating temperature range: -55C to 40C</li> </ul>
11*	Soil Sensor (Valence state, molecular structure, & properties of rocks)	Mössbauer Spectrometer	<ul style="list-style-type: none"> <li>- Reveal valence state, molecular structure, &amp; magnetic properties of iron-bearing minerals &amp; rocks</li> <li>- Determine oxidation state</li> <li>- Identify iron oxides and magnetic phase in soil, Fe-bearing minerals in rocks, search for Fe-sulfates, nitrates and carbonates</li> <li>- used in the MER rovers</li> <li>- operating temperature range: -55C to 40C</li> </ul>
12*	Moisture Sensor (water content of shallow surface)	Neutron Spectrometer System (NSS)	<ul style="list-style-type: none"> <li>- Identify locations of enhanced hydrogen content as low as 0.5% equivalent hydrogen</li> <li>- operating temperature range: -40C to 60C</li> </ul>
13	Batteries	COTS 18560 Li-ion cells	<ul style="list-style-type: none"> <li>- Rechargeable</li> <li>- Positive thermal coefficient (PTC) limits the current</li> <li>- Current-interrupt device (CID) safeguards against overcharge</li> <li>- Shut-down separators eliminate ion transport channels at higher temperatures</li> <li>- typical batteries operate at -20C to 60C</li> </ul>
14	Solar Panels	InGaP/GaAs/Ge Solar Cell	<ul style="list-style-type: none"> <li>- 32.3% efficiency</li> <li>- Spectrolab Space Voltaics: designed to withstand extreme temperature conditions encountered in space environments</li> </ul>

\*made up of COTS components

\*\*custom-made for mission

## E. CAD Models

Detailed CAD models of the fully assembled A.L.I.C.E including the isometric and orthographic views are shown in Figure 8.



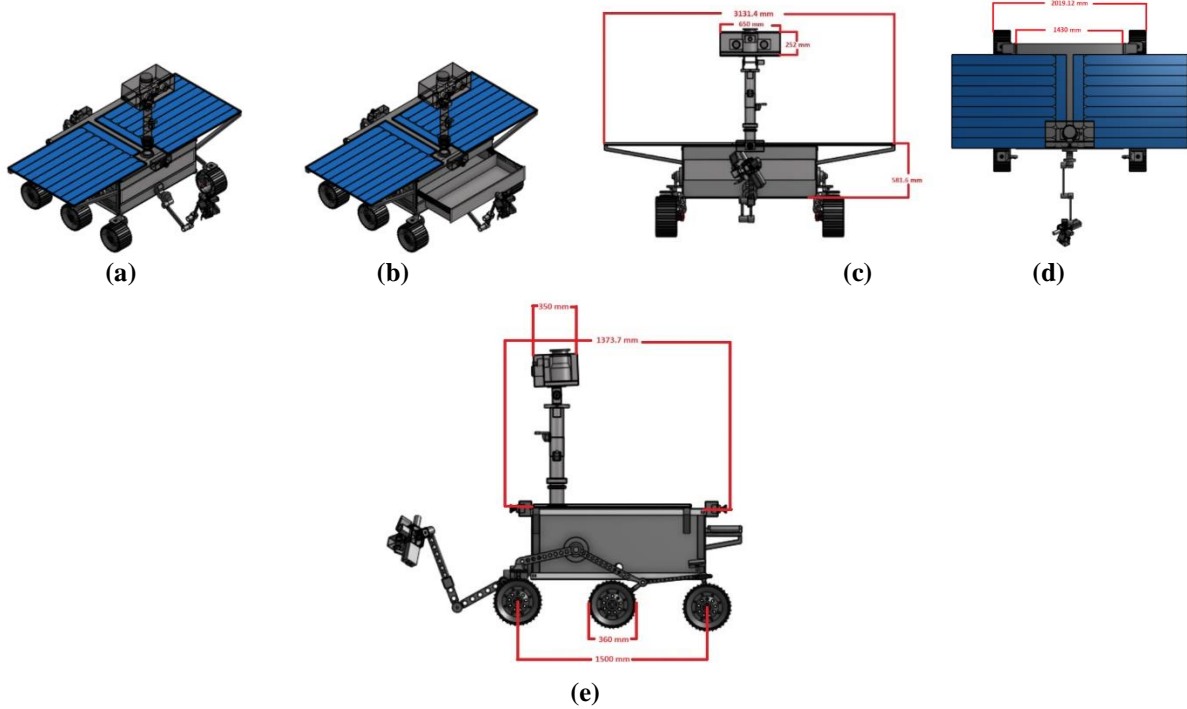


**Fig. 8 (a) Isometric View of A.L.I.C.E.: Retracted, (b) Isometric View of A.L.I.C.E.: Extended, (c) Front View of A.L.I.C.E. (middle left), (d) Top View of A.L.I.C.E. (middle right), (e) Right-Side View of A.L.I.C.E. (bottom)**

The pole and the robotic arm are shown in Figure 8. The placement of the Pancams, REMS, and the Radiation Assessment Detector are all on the pole, while the Mossbauer Spectrometer, APXS, Rock Abrasion Tool, and Microscopic Imager are on the robotic arm, along with a pick and shovel for sample collection.

From the top view shown in Figure 8d, the solar panels consisting of Spectrolab solar voltaic cells and an overhead picture of the Radiation Assessment Detector can be seen. The rotation capability of the four instruments on the robotic arm can be inferred from its position.

The rocker-bogie suspension system is revealed when looking at the rover from a side view. The rocker-bogie system has two parts (rocker and bogie) which allows the wheels to climb over larger objects without compromising stability.

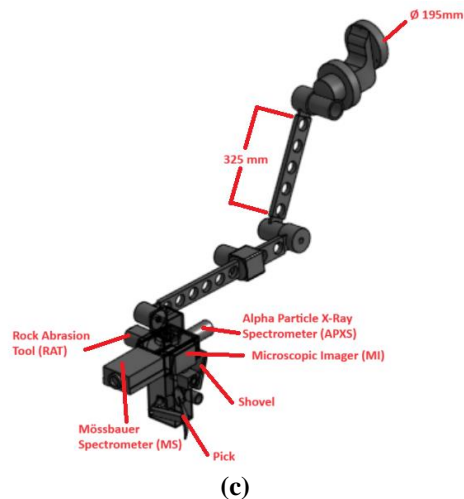


**Fig. 9 Isometric View of Robotic Arm**

The Robotic Arm as shown in Figures 9 and 10 includes two joints from a mount that attaches to the front face of the rover. The end of the arm holds four different instruments, along with a pick and shovel for sample collection.

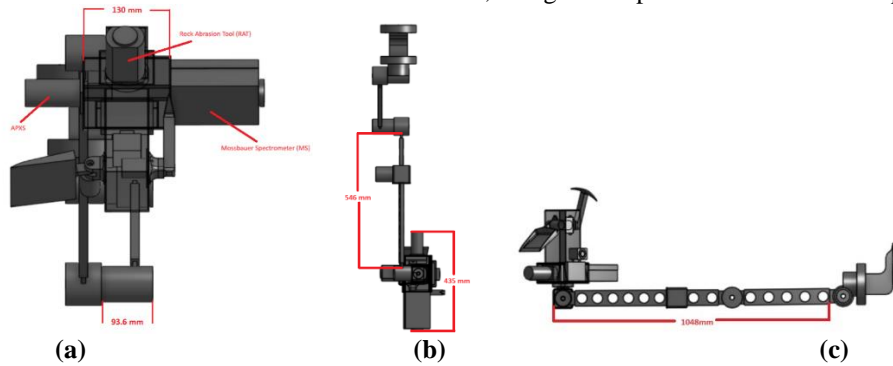


**Fig. 10 (a) Front View of Robotic Arm (top left), (b) Top View of Robotic Arm (top right), (c) Side View of Robotic Arm - Full Extension (bottom)**

The four instruments seen on the robotic arm are the Alpha Particle X-Ray Spectrometer (APXS), Mossbauer Spectrometer (MS), Microscopic Imager (MI), and the Rock Abrasion Tool (RAT).

The pick and shovel allow for sample collection and storage. Storage drawers are shown in Figure 12 both in open and closed positions. When other instruments are in use, both can bend upwards to get out of the way.

The robotic arm is mounted to the front of the rover to allow for unrestricted movement in its surroundings.

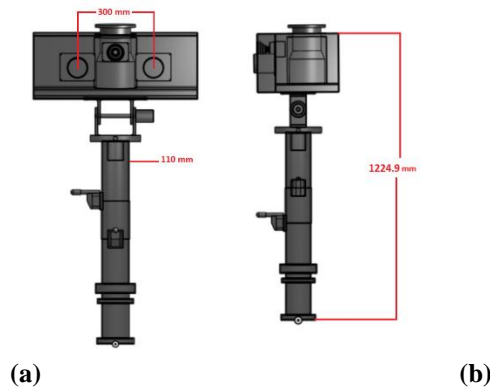


**Fig. 11 (a) Front View of Pole (left), (b) Side View of Pole (right)**

The pole includes two Panoramic Cameras and the Navigation Camera at the head as well as the Radiation Assessment Detector (RAD) as shown in Figure 11. The head is able to move 360 degrees in yaw, and 180 degrees in pitch.

The pole also acts as an attachment for the Rover Environmental Monitoring Station (REMS). It has sensors for wind, temperature, and humidity on the lunar surface.

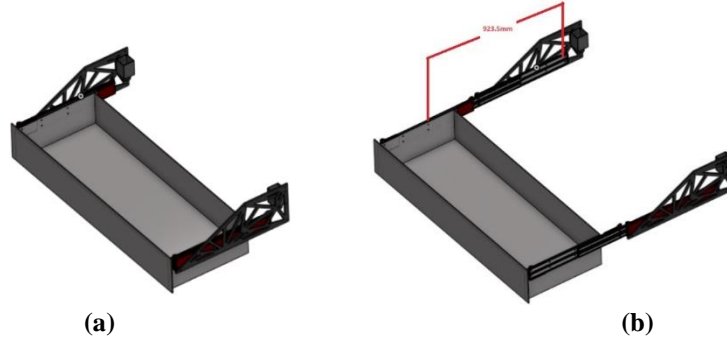


**Fig. 12 (a) Isometric View of Sample Storage Drawer (left), (b) Isometric View of Extended Sample Storage Drawer (right)**

## F. Analysis

In this section, the Finite Element Analysis (FEA) and results are discussed. This includes the analysis performed shovel and robotic arm, which is vital to understand if the system is properly supported.

### i. Robotic Arm

The density of the soil on the lunar surface is about  $1.5 \text{ g/cm}^3$ , or  $1500 \text{ kg/m}^3$ . The largest side of the interior of the shovel has a length of 96mm and corresponds to a radius of 0.048m. With this information, the mass of a theoretical cone-shaped sample was calculated:

$$\begin{aligned}
 m &= DV \\
 m &= 1500 * \left(\frac{1}{3}\pi r^2 h\right) \\
 m &= 1500 * \left(\frac{1}{3}\pi(0.048)^2(0.048 \tan(80^\circ))\right) \\
 m &= 1500 * \left(\frac{1}{3}\pi(0.048)^2(0.272)\right) \\
 m &= 1500 * (6.56 * 10^{-4}) \\
 m &= 0.99 \text{ kg}
 \end{aligned}$$

The gravitational field strength on the Moon is  $1.625 \text{ m/s}^2$ . Using Newton's Second Law, the amount of force the sample exerts on the shovel can be found:

$$\begin{aligned}
 F &= ma \\
 F &= (0.99)(1.625) \\
 F &= 1.61 \text{ N}
 \end{aligned}$$

For the purpose of the analysis, this value was rounded up to 2N. With an additional safety factor of 2, the robotic arm was tested with a force value of 4N. The distributed force applied on the shovel when the arm is fully extended is shown in Figure 13a. The Von Mises stress obtained in the arm as a result of this force is shown in Figure 13b and the displacement is shown in Figure 13c.

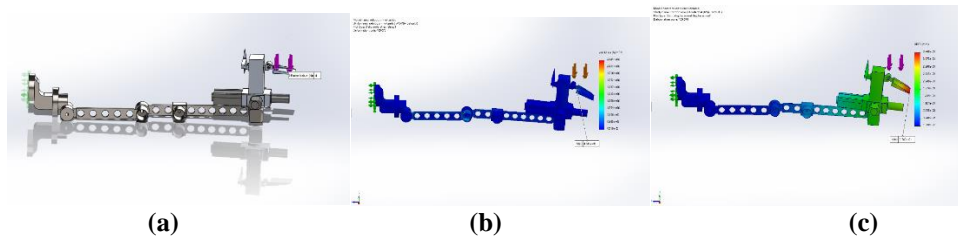


**Fig. 13 (a) Applied Forces, (b) Von Mises Stress, (c) Displacement**

The maximum value for the Von Mises Stress is  $4.645 \times 10^6 \text{ N/m}^2$ , located at the shovel handle. This is less than the yield strength of the material used (Aluminum 6065). This analysis verifies that under the maximum load condition, the as designed arm will be able to withhold this load without failure. The maximum value for the Displacement is  $3.748 \times 10^{-1} \text{ mm}$ , located at the tip of the shovel where the sample is held.

## References

- [1] J. Zakrajsek *et al.*, “First AIAA Space Exploration Conference Exploration Rover Concepts and Development Challenges,” 2005. Available: [https://www.nasa.gov/sites/default/files/atoms/files/exploration\\_rover\\_concepts\\_grc.pdf](https://www.nasa.gov/sites/default/files/atoms/files/exploration_rover_concepts_grc.pdf)
- [2] S. Kassel, “Lunokhod-1 Soviet Lunar Surface Vehicle A Report prepared for,” Jun. 1971. Available: <https://apps.dtic.mil/sti/pdfs/AD0733960.pdf>
- [3] V. Gromov *et al.*, “LUNOKHOD 2 – A RETROSPECTIVE GLANCE AFTER 30 YEARS,” *ResearchGate*, 2003. [https://www.researchgate.net/profile/Mikhail-Malenkov/publication/234403845\\_Lunokhod\\_2\\_-\\_A\\_retrospective\\_Glance\\_after\\_30\\_Years/links/60c502a14585157774d22ca7/Lunokhod-2-A-retrospective-Glance-after-30-Years.pdf](https://www.researchgate.net/profile/Mikhail-Malenkov/publication/234403845_Lunokhod_2_-_A_retrospective_Glance_after_30_Years/links/60c502a14585157774d22ca7/Lunokhod-2-A-retrospective-Glance-after-30-Years.pdf)
- [4] B. Wilcox and T. Nguyen, “Sojourner on Mars and Lessons Learned for Future Planetary Rovers,” *dataverse.jpl.nasa.gov*, 1998. <https://dataverse.jpl.nasa.gov/file.xhtml?fileId=43308&version=1.0>
- [5] M. Maimone, J. Biesiadecki, E. Tunstel, Y. Cheng, and C. Leger, “Chapter 3 SURFACE NAVIGATION AND MOBILITY INTELLIGENCE ON THE MARS EXPLORATION ROVERS,” 2006. Available: [https://www-robotics.jpl.nasa.gov/media/documents/05\\_Chapter3\\_final.pdf](https://www-robotics.jpl.nasa.gov/media/documents/05_Chapter3_final.pdf)
- [6] J. A. Crisp, M. Adler, J. R. Matijevic, S. W. Squyres, R. E. Arvidson, and D. M. Kass, “Mars Exploration Rover mission,” *Journal of Geophysical Research: Planets*, vol. 108, no. E12, Oct. 2003, doi: <https://doi.org/10.1029/2002je002038>.
- [7] J. Purvis and P. Klarer, “Robotic All-Terrain Lunar Exploration Rover,” 1993. Accessed: 2023. [Online]. Available: <https://ntrs.nasa.gov/api/citations/19930022928/downloads/19930022928.pdf>
- [8] W. A. Amai, P. R. Klarer, J. B. Pletta, J. W. Purvis, and R. P. Case, “Robotic all-terrain lunar exploration rover (RATLER) FY93 program status report,” *www.osti.gov*, Oct. 01, 1994. <https://www.osti.gov/servlets/purl/10196260> (accessed 2023).
- [9] “NASA - NSSDCA - Spacecraft - Details,” *nssdc.gsfc.nasa.gov*, 2018. <https://nssdc.gsfc.nasa.gov/nmc/spacecraft/display.action?id=2018-103A>
- [10] J. N. Maki *et al.*, “Mars Exploration Rover Engineering Cameras,” *Journal of Geophysical Research: Planets*, vol. 108, no. E12, Dec. 2003, doi: <https://doi.org/10.1029/2003je002077>.
- [11] J. Gómez-Elvira *et al.*, “Curiosity’s rover environmental monitoring station: Overview of the first 100 sols,” *Journal of Geophysical Research: Planets*, vol. 119, no. 7, pp. 1680–1688, Jul. 2014, doi: <https://doi.org/10.1002/2013je004576>.
- [12] S. W. Squyres *et al.*, “Athena Mars rover science investigation,” *Journal of Geophysical Research: Planets*, vol. 108, no. E12, Dec. 2003, doi: <https://doi.org/10.1029/2003je002121>.
- [13] M. Schrön *et al.*, “The Cosmic-Ray Neutron Rover - Mobile Surveys of Field Soil Moisture and the Influence of Roads,” *Water Resources Research*, vol. 54, no. 9, Sep. 2018, doi: <https://doi.org/10.1029/2017wr021719>.
- [14] J. F. Bell *et al.*, “The Mars Science Laboratory Curiosity rover Mastcam instruments: Preflight and in-flight calibration, validation, and data archiving,” *Earth and Space Science*, vol. 4, no. 7, pp. 396–452, Jul. 2017, doi: <https://doi.org/10.1002/2016ea000219>.
- [15] J. A. Rodriguez-Manfredi *et al.*, “The Mars Environmental Dynamics Analyzer, MEDA. A Suite of Environmental Sensors for the Mars 2020 Mission,” *Space Science Reviews*, vol. 217, no. 3, Apr. 2021, doi: <https://doi.org/10.1007/s11214-021-00816-9>.
- [16] D. J. McCleese *et al.*, “Mars Climate Sounder: An investigation of thermal and water vapor structure, dust and condensate distributions in the atmosphere, and energy balance of the polar regions,” *Journal of Geophysical Research*, vol. 112, no. E5, May 2007, doi: <https://doi.org/10.1029/2006je002790>.
- [17] R. Ramesham, J. N. Maki, and G. C. Cucullu, “Qualification Testing of Engineering Camera and Platinum Resistance Thermometer (PRT) Sensors for MSL Project Under Extreme Temperatures to Assess Reliability and to Enhance Mission Assurance,” *Journal of Microelectronics and Electronic Packaging*, vol. 6, no. 2, pp. 125–134, Apr. 2009, doi: <https://doi.org/10.4071/1551-4897-6.2.125>.

- [18] G. Quattrocchi, A. Pittari, M. D.L. dalla Vedova, and P. Maggiore, “The thermal control system of NASA’s Curiosity rover: a case study,” in *IOP Conference Series: Materials Science and Engineering*, 2022. Accessed: 2023. [Online]. Available: <https://iopscience.iop.org/article/10.1088/1757-899X/1226/1/012113/meta>
- [19] R. Gaza, M. Kroupa, R. Rios, N. Stoffle, E. R. Benton, and E. J. Semones, “Comparison of novel active semiconductor pixel detector with passive radiation detectors during the NASA Orion Exploration Flight Test 1 (EFT-1),” *Radiation Measurements*, vol. 106, pp. 290–297, Mar. 2017, doi: <https://doi.org/10.1016/j.radmeas.2017.03.041>.
- [20] J. Gómez-Elvira *et al.*, “REMS: The Environmental Sensor Suite for the Mars Science Laboratory Rover,” *Space Science Reviews*, vol. 170, no. 1–4, pp. 583–640, Aug. 2012, doi: <https://doi.org/10.1007/s11214-012-9921-1>.
- [21] R. Surampudi *et al.*, “Energy Storage Technologies for Future Planetary Science Missions,” 2017. Accessed: Jun. 22, 2023. [Online]. Available: [https://solarsystem.nasa.gov/system/downloadable\\_items/716\\_Energy\\_Storage\\_Tech\\_Report\\_FINAL.PDF](https://solarsystem.nasa.gov/system/downloadable_items/716_Energy_Storage_Tech_Report_FINAL.PDF)
- [22] F. C. Krause *et al.*, “Performance of Commercial Li-Ion Cells for Future NASA Missions and Aerospace Applications,” *Journal of the Electrochemical Society*, 2021, Accessed: 2023. [Online]. Available: <https://iopscience.iop.org/article/10.1149/1945-7111/abf05f/pdf>
- [23] J. P. Jones, M. C. Smart, F. C. Krause, W. C. West, and E. J. Brandon, “Batteries for robotic spacecraft,” *Joule*, vol. 6, no. 5, pp. 923–928, May 2022, doi: <https://doi.org/10.1016/j.joule.2022.04.004>.
- [24] R. V. Bugga and E. J. Brandon, “Energy Storage for the Next Generation of Robotic Space Exploration,” *The Electrochemical Society Interface*, vol. 29, no. 1, pp. 59–63, Mar. 2020, doi: <https://doi.org/10.1149/2.f08201if>.
- [25] F. Cordes, C. Oekermann, A. Babu, D. Kuehn, T. Stark, and F. Kirchner, “An Active Suspension System for a Planetary Rover,” 2014. [https://www.dfki.de/fileadmin/user\\_upload/import/7261\\_20140617\\_iSAIRAS14\\_CordesEtAl\\_ActiveSuspensionPlanetaryRover.pdf](https://www.dfki.de/fileadmin/user_upload/import/7261_20140617_iSAIRAS14_CordesEtAl_ActiveSuspensionPlanetaryRover.pdf) (accessed 2023).
- [26] S. Gerdtts, J. Breckenridge, and K. P. Johnson, “Lunar Rover Optimization Platform for Wheel Traction Studies,” Apr. 2021, doi: <https://doi.org/10.1061/9780784483374.038>.
- [27] D. Braun and D. Noon, “‘Long Life’ DC brush motor for use on the Mars Surveyor Program,” *dataverse.jpl.nasa.gov*, 1998. <https://dataverse.jpl.nasa.gov/file.xhtml?fileId=25719&version=1.0> (accessed Jun. 22, 2023).
- [28] L. K. Ding *et al.*, “A 2-year locomotive exploration and scientific investigation of the lunar farside by the Yutu-2 rover,” vol. 7, no. 62, Jan. 2022, doi: <https://doi.org/10.1126/scirobotics.abj6660>.
- [29] T. V. Torchynska and G. Polupan, “High efficiency solar cells for space applications,” *Superficies y vacío*, vol. 17, no. 3, 2004, Accessed: 2023. [Online]. Available: <https://www.redalyc.org/pdf/942/94217305.pdf>
- [30] G. Landis, T. Kerslake, D. Scheiman, and P. Jenkins, “Mars Solar Power,” *2nd International Energy Conversion Engineering Conference*, 2004, doi: <https://doi.org/10.2514/6.2004-5555>.
- [31] D. Schmanke, G. Klingelhöfer, J. Girones Lopez, J. Brückner, and C. d’Uston, “The Alpha Particle X-Ray Spectrometer APXS on the Rosetta lander Philae to explore the surface of comet 67P/Churyumov-Gerasimenko,” 2010. Accessed: 2023. [Online]. Available: <https://meetingorganizer.copernicus.org/EPSC2010/EPSC2010-898.pdf>
- [32] “NASA - NSSDCA - Experiment - Details,” *nssdc.gsfc.nasa.gov*, 2003. <https://nssdc.gsfc.nasa.gov/nmc/experiment/display.action?id=2003-027A-06> (accessed Jun. 25, 2023).
- [33] “Mössbauer Spectrometer (MB),” *Wustl.edu*, 2023. <https://an.rsl.wustl.edu/help/Content/About%20the%20mission/MER/Instruments/Moessbauer%20Spectrometer.htm> (accessed Jun. 25, 2023).
- [34] J. Mondt, K. Burke, B. Bragg, G. Rao, and S. Vukson, “Energy Storage Technologies for Future Space Science Missions,” *NASA Solar System Exploration*, 2004. <https://solarsystem.nasa.gov/resources/295/energy-storage-technologies-for-future-space-science-missions/> (accessed Jun. 29, 2023).
- [35] P. N. Peplowski, R. C. Elphic, E. L. Fritzler, and J. T. Wilson, “Calibration of NASA’s Neutron Spectrometer System (NSS) for landed measurements of hydrogen content of the lunar subsurface,” *Nuclear Instruments and Methods in Physics Research Section A: Accelerators, Spectrometers, Detectors and Associated Equipment*, vol. 1049, p. 168063, Apr. 2023, doi: <https://doi.org/10.1016/j.nima.2023.168063>.
- [36] NASA, “Sensor on Mars Rover to Measure Radiation Environment,” *NASA Mars Exploration*, Nov. 09, 2010. [https://mars.nasa.gov/news/1081/sensor-on-mars-rover-to-measure-radiation-environment/#:~:text=The%201.7%2Dkilogram%20\(3.8%2D](https://mars.nasa.gov/news/1081/sensor-on-mars-rover-to-measure-radiation-environment/#:~:text=The%201.7%2Dkilogram%20(3.8%2D) (accessed Jul. 10, 2023).